Superconductivity in $Cu_xBi_2Se_3$ and its Implications for Pairing in the Undoped Topological Insulator

Y. S. Hor,[1] A. J. Williams,[1] J. G. Checkelsky,[2] P. Roushan,[2] J. Seo,[2] Q. Xu,[3] H. W. Zandbergen,[3] A. Yazdani,[2] N. P. Ong,[2] and R. J. Cava[1]

[1]*Department of Chemistry, Princeton University, Princeton, New Jersey 08544, USA*
[2]*Department of Physics, Princeton University, Princeton, New Jersey 08544, USA*
[3]*National Centre for HREM, Department of Nanoscience, Delft Institute of Technology, 2628 CJ Delft, The Netherlands*

(Received 6 October 2009; published 1 February 2010)

Bi_2Se_3 is one of a handful of known topological insulators. Here we show that copper intercalation in the van der Waals gaps between the Bi_2Se_3 layers, yielding an electron concentration of $\sim 2 \times 10^{20}$ cm^{-3}, results in superconductivity at 3.8 K in $Cu_xBi_2Se_3$ for $0.12 \leq x \leq 0.15$. This demonstrates that Cooper pairing is possible in Bi_2Se_3 at accessible temperatures, with implications for studying the physics of topological insulators and potential devices.

DOI: 10.1103/PhysRevLett.104.057001 PACS numbers: 74.70.−b, 73.20.At, 74.10.+v, 74.90.+n

Topological insulators display conducting surface states that are a distinct electronic phase of matter, with photonlike energy dispersions, stabilized even at high temperatures due to the topology of the system [see, e.g., [1–3]]. Theoretical interest in topological surface states is high, stimulated by their observation in HgTe-based quantum wells [4,5] and the prediction [6,7] and then observation [8] that they are present on the surface of bulk Bi-Sb alloy crystals. Topological surface states have recently been observed in a second bulk materials class, Bi_2Se_3 and Bi_2Te_3 [9,10]. Several schemes have been proposed to search for novel electronic excitations of the surface states, particularly Majorana fermions [11], which are potentially useful for topological quantum computing [e.g., [12–18]]. All the proposed schemes rely on the opening of an energy gap in the surface state spectrum by inducing superconductivity through the proximity effect. However, Cooper pairing of electrons at accessible temperatures in a topological insulator has never been reported. Here we show that the topological insulator Bi_2Se_3 can be made into a superconductor by Cu intercalation. This implies that Cooper pairing can occur in Bi_2Se_3 up to about 4 K. Because of their intrinsic chemical and structural compatibility, electronic junctions between Bi_2Se_3 and $Cu_xBi_2Se_3$ are feasible. Such junctions are promising for investigating novel concepts in physics as well as for new types of electronic devices.

Bi_2Se_3 [19] is made from double layers of $BiSe_6$ octahedra [Fig. 1(a)]. The resulting Se-Bi-Se-Bi-Se five layer sandwich is only weakly van der Waals bonded to the next sandwich, through the outer Se layers, yielding a material with excellent basal plane cleavage and excellent quality layered crystals both in the bulk and in thin films [19–21]. This layered nature results in the fact that both substitutional and intercalative chemical manipulations are possible. The dopant employed here, Cu, may either intercalate between the Se layers, as it does in Cu_xTiSe_2 [22], or randomly substitute for Bi within the host structure, as has been reported for the NaCl structure compound $CuBiSe_2$ [23]. This dual nature was recognized early on in Cu doping studies of Bi_2Se_3 [24,25], where substantial differences in the electrical properties of Cu-substituted $Bi_{2-x}Cu_xSe_3$ and Cu-intercalated $Cu_xBi_2Se_3$ were reported and it was concluded that Cu acts as an ambipolar dopant.

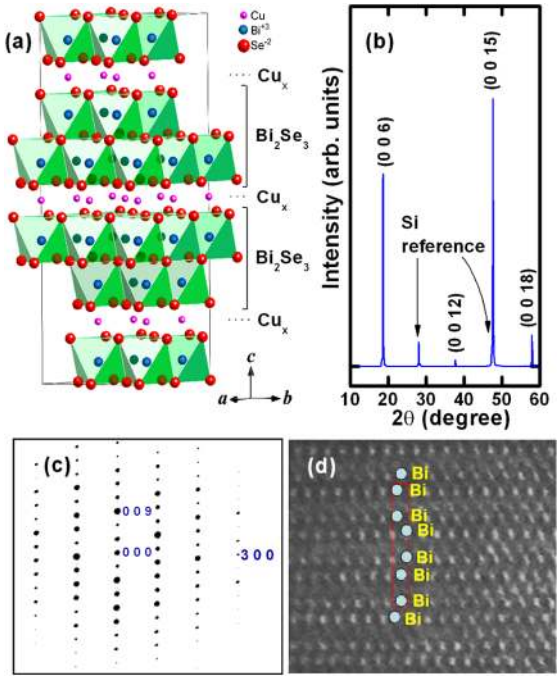

FIG. 1 (color online). (a) The crystal structure of Cu intercalated Bi_2Se_3. (b) X-ray diffraction scan showing the $00L$ reflections from the basal plane of a cleaved $Cu_{0.12}Bi_2Se_3$ single crystal with Si powder diffraction as a calibration. (c) The $\langle 110 \rangle$ zone axis electron diffraction pattern for $Cu_{0.12}Bi_2Se_3$. (d) High resolution electron microscope image of a representative area of $Cu_{0.12}Bi_2Se_3$, showing the regular array of layers (labeled by atom type) and the absence of stacking defects on the nanoscale.

Whether Cu is incorporated by intercalation or substitution in Bi_2Se_3 is nominally controlled by the elemental ratios, but because both kinds of incorporation are possible, the precise distribution of Cu between intercalated and substituted sites strongly processing dependent, a factor that we find to be a significant influence on the presence of the superconductivity.

Single crystals of $Cu_xBi_2Se_3$ and $Bi_{2-x}Cu_xSe_3$ were grown by melting stoichiometric mixtures of Bi (99.999%), Cu (99.99%), and Se (99.999%) at 850 °C overnight in sealed evacuated quartz tubes. The crystal growth took place via slow cooling from 850 to 620 °C and then quenching in cold water. The resultant crystals are easily cleaved along the basal plane leaving a silvery shining mirror like surface. The silvery surfaces of $Cu_xBi_2Se_3$ turn golden after one day exposure to air, suggesting that exposure to air should be kept to a minimum.

The crystal structure of the $Cu_xBi_2Se_3$ crystals was confirmed by x-ray powder diffraction using a Bruker D8 diffractometer with Cu $K\alpha$ radiation. High resolution electron microscopy (HREM) analysis was performed with a Philips CM300UT electron microscope operating at 300 kV. Scanning tunneling microscopy measurements were performed in a home-built cryogenic scanning tunneling microscope (STM) operated at 4.2 K in ultrahigh vacuum. The samples were cleaved *in situ* to expose a pristine surface.

Resistivity and ac magnetization measurements were performed in a quantum design physical property measurement system (PPMS). The standard four-probe technique, employing silver paste contacts cured at room temperature, was used for resistivity measurements, with the electric currents applied in the basal plane of the crystals. Hall effect measurements were performed in a home-built apparatus 0.3 and 15 K. A quantum design superconducting quantum interference device (SQUID) was used to measure dc magnetization.

Single crystals of $Bi_{2-x}Cu_xSe_3$ prepared for $x = 0$ to 0.15 were never superconducting. In contrast, single crystals of $Cu_xBi_2Se_3$ within the composition range $0.10 < x < 0.15$ were reproducibly superconducting. An x-ray diffraction scan of the basal plane reflections from a single crystal of superconducting $Cu_{0.12}Bi_2Se_3$ is shown in Fig. 1(b). This scan shows that the single crystal is chemically single phase, and further shows several of the $00L$ reflections obeying the expected systematic absences for the rhombohedral space group of Bi_2Se_3 [19]. The reflections are very sharp, indicating excellent crystalline quality on the long range. For $Cu_xBi_2Se_3$ crystals, we observe a significant increase in the c-axis lattice parameter (the layer stacking direction), from $c = 28.666(1)$ Å for Bi_2Se_3, to $c = 28.736(1)$ Å for $Cu_{0.12}Bi_2Se_3$ for example. We infer, by analogy to the behavior in related layered selenides [22], that the intercalated Cu in the van der Waals gap partially occupies the octahedrally coordinated $3b$ $(0, 0, \frac{1}{2})$ sites in the $R\bar{3}m$ space group, shown in Fig. 1(a). Electron diffraction [Fig. 1(c)] and HREM [Fig. 1(d)] in zones including the c^* stacking axis, taken from many fragments of $Cu_xBi_2Se_3$, showed no sign of stacking faults, intergrowths, or amorphous regions, indicating that the quality of the crystals is good on the nanoscale. None of the diffraction experiments indicated the presence of long or short range ordering of the Cu in the interstitial sites. The single crystals at the optimal superconducting composition are therefore single phase with excellent long range and nanoscale crystallinity.

Magnetic characterization of the superconducting transition in $Cu_{0.12}Bi_2Se_3$ is shown in the main panel of Fig. 2. T_c is approximately 3.8 K. The magnetization observed at the lowest temperature of the zero field cooled (ZFC) measurement on the single crystal is about 20% of that expected for full diamagnetism. This represents a conservative lower limit to the true superconducting volume fraction because the diamagnetic magnetization is still decreasing steeply at the temperature where the field is applied for the ZFC measurement. Superconductivity was observed only in a narrow window of x in $Cu_xBi_2Se_3$, for $0.1 \leq x \leq 0.3$, with the optimal single crystal compositions between $x = 0.12$ and $x = 0.15$ (inset Fig. 2). Small deviations of Se stoichiometry from 3.00/formula unit suppress the superconductivity. For nominal x greater than 0.15 in $Cu_xBi_2Se_3$ melts, pure single crystals were not obtained. The minor impurity phases present were Cu_2Se and $CuBi_3Se_5$ (also reported as $Cu_{1.6}Bi_{4.8}Se_8$ [26]). Samples of these phases, and many other compositions in the Cu-Bi-Se system, $CuBiSe_2$ [23] and $BiCu_3Se_3$ [27], as well as compositions deviating from the stoichiometry $Cu_xBi_2Se_3$ for $0.10 \leq x \leq 0.30$ were tested and found to be nonsuperconducting above 1.8 K (upper inset Fig. 2). Thus the observed superconductivity is unambiguously identified with $Cu_xBi_2Se_3$. The temperature dependence of the upper critical field, H_{c2}, determined from resistivity (see below), is shown in the lower inset of Fig. 2. At 0.3 K, H_{c2} is 1.7 T and 4.6 T for the field parallel to the c axis, $H \parallel c$, and parallel to the basal plane, $H \parallel ab$, respectively. $Cu_xBi_2Se_3$ is a strongly type II superconductor with a Ginzburg-Landau parameter $\kappa \sim 50$. The inferred coherence lengths ($\xi_c = 52$ Å, $\xi_{ab} = 140$ Å) imply a pair condensate with a moderately large anisotropy (~ 3).

Figure 3 shows the temperature dependence of the resistivity for $Cu_{0.12}Bi_2Se_3$, measured in the ab plane. The resistivity is weakly metallic. Hall effect measurements indicated that this crystal is n type, with a temperature independent (between 4 and 300 K) carrier density $\sim 2 \times 10^{20}$ cm^{-3}, comparable to what has been observed previously for $Cu_xBi_2Se_3$ [25]. This carrier concentration is 1 order of magnitude higher than is found in native Bi_2Se_3 [24,25], and 2 orders of magnitude higher than is found for crystals with chemical potentials tuned into the gap region by Ca doping [28,29]. The Seebeck coefficient for superconducting $Cu_xBi_2Se_3$ is negative and smaller

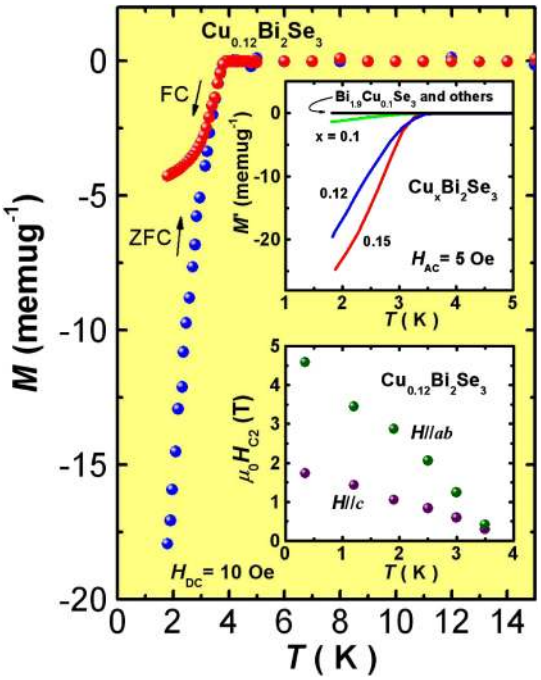

FIG. 2 (color online). The temperature dependent magnetization of a single crystal of $Cu_{0.12}Bi_2Se_3$ shows a superconducting transition $T_c \sim 3.8$ K in zero field cooled (ZFC) and field cooled (FC) measurements. Upper inset: superconductivity occurs only in a narrow window of x in $Cu_xBi_2Se_3$. Superconductivity is not found for $x < 0.1$ and $x > 0.3$, or in $Bi_{2-x}Cu_xSe_3$, Cu_2Se, $CuBi_3Se_5$, $BiCuSe_2$, and $BiCu_3Se_3$ (data labeled in inset as "$Bi_{1.9}Cu_{0.1}Se_3$ and others"). Lower inset: temperature dependence of the superconducting upper critical field, $H_{c2}(T)$ of $Cu_{0.12}Bi_2Se_3$ for the magnetic field applied parallel to the c axis and parallel to the ab plane.

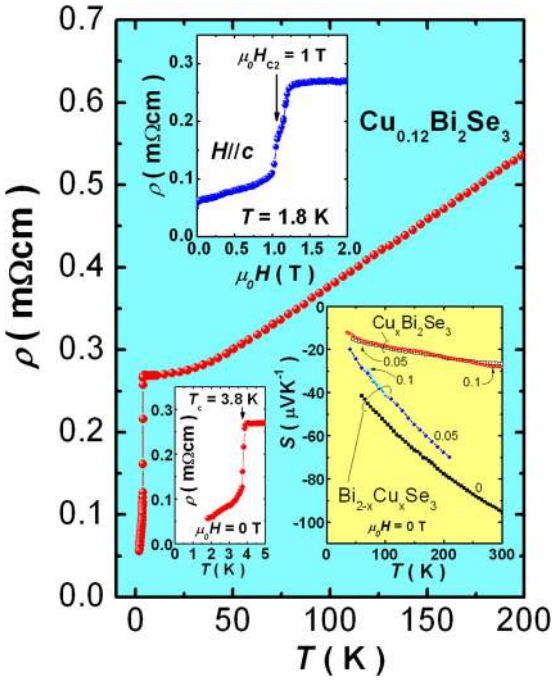

FIG. 3 (color online). The resistivity of a $Cu_{0.12}Bi_2Se_3$ crystal with applied current in the ab plane. The lower inset shows that the superconducting transition occurs at ~3.8 K. The upper inset shows the magnetoresistance plot at $T = 1.8$ K for the field applied parallel to the c axis. An upper critical field of $\mu_o H_C \sim 1$ T is observed. The third inset shows the comparison of the Seebeck coefficients of $Cu_xBi_2Se_3$ and $Bi_{2-x}Cu_xSe_3$.

than found in the undoped material (inset Fig. 3), consistent with the much larger number of n-type carriers observed in the Hall effect measurements. The superconducting transition (lower left inset Fig. 3), occurs at 3.8 K. The resistivity does not drop to zero below T_c however, indicating the absence of a continuous superconducting path. This is contrary to what is generally seen in superconducting materials, where a continuous zero resistance path is often present even when the superconducting volume fraction is small. We attribute this to the sensitivity of the superconducting phase to processing and stoichiometry, which yields weak links and low critical currents in the crystals. The origin of this sensitivity is likely the chemical stability of both superconducting $Cu_xBi_2Se_3$ and nonsuperconducting $Bi_{2-x}Cu_xSe_3$, which are electrically quite different (e.g., lower right inset Fig. 3); the distinction between these two materials is difficult to control in the synthesis. Resistivity data showing the suppression of superconductivity in an applied field (upper inset Fig. 3) were employed to determine the $H_{c2}(T)$ behavior presented in Fig. 2.

The structural and electronic character of the Cu intercalant in Bi_2Se_3 is of particular interest. To investigate this at the nanometer scale, we studied the (001) surface of a cleaved $Cu_{0.15}Bi_2Se_3$ single crystal using an STM at 4.2 K. Several distinct features can be identified in the STM topographic images. Figure 4 shows topographies of filled and unoccupied states over an area of size 250 Å by 250 Å. One feature (type 1), with an apparent height of ~2 to 3 Å, occurs in different shapes and sizes, and appears as red or orange regions in Fig. 4. From the height of these features and their shapes, we conclude that they are located on the cleaved surface and are clusters of intercalated Cu atoms that have formed on the surface of the cleaved crystal by surface diffusion. A second feature (type 2) appears as a bright triangular area, yellow in Fig. 4, of lateral dimension ~20 Å. We associate these features with intercalated Cu in subsurface van der Waals gap layers. They have a symmetry-defined shape. Hence there is no evidence of Cu cluster formation below the exposed surface, and the copper is seen to have a random distribution in the superconducting phase, consistent with the TEM characterization. Neither of these features is present in native or Ca-doped Bi_2Se_3 [28] and thus they are clearly associated with the Cu intercalation. Because these topographic features have similar appearance in both filled and unoccupied state topographies in the STM images, Cu is not uniquely a donor or acceptor in this system consistent with conclusions drawn from transport studies [24,25]. Our Hall effect and Seebeck coefficient data indicate that n-type carriers

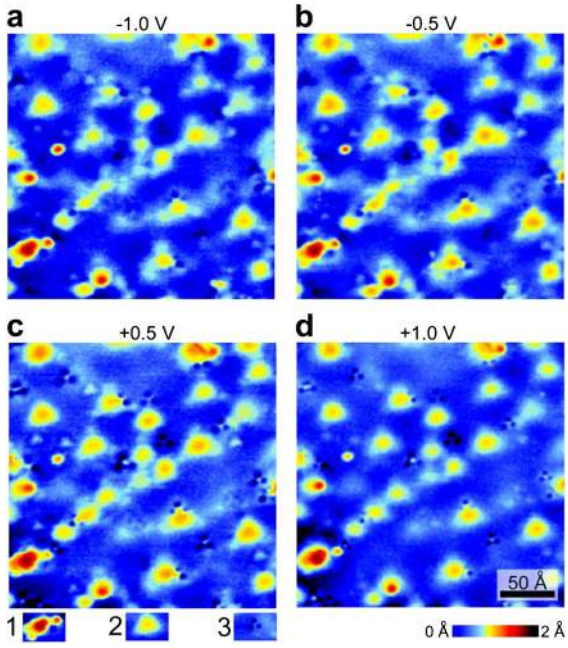

FIG. 4 (color online). STM topographic images over a 250 Å by 250 Å area showing the filled states at bias voltages of (a) −1.0 V and (b) −0.5 V; and the unoccupied states at bias voltages of (c) +0.5 V and (d) +1.0 V. Three types of topological features are identified, denoted as 1, 2, and 3 in the legend. Type 1 and type 2 features are identified as Cu on the cleaved surface and intercalated in van der Waals layers beneath the surface, respectively.

dominate the transport at the superconducting composition, however, so the net result of the Cu intercalation is to generate mobile electrons in the conduction band. A third feature (type 3), also having a threefold symmetry, (visible, for example, as a triangle of dark circles in the +1 V image in Fig. 4), but with bias dependence, is also present. Unambiguous identification of this feature will require further study.

Previous experimental and theoretical work on Bi_2Se_3 suggests that it may be the most interesting of the bulk topological insulators known to date because it can in fact be made resistive in the bulk through doping and also because only topological surface states are present [28–31]. We have here shown that $Cu_xBi_2Se_3$ displays superconductivity at accessible temperatures in the doping range $0.12 \leq x \leq 0.15$, adding an important attribute to the favorable characteristics of this system.

Most proposals to manipulate the topological surface states in Bi_2Se_3 rely on the opening of a superconducting gap by proximity to a superconductor. Our result, showing that pairing exists up to 3.8 K (albeit at a density of 2×10^{20} cm^{-3}), provides strong impetus to these efforts. As $Cu_xBi_2Se_3$ and Bi_2Se_3 are chemically closely similar, supercurrents should readily tunnel between them. Furthermore, if modulation doping is achieved by atomic-scale control of the Cu sites (e.g., by molecular-beam epitaxy), we anticipate novel device structures based on having superconducting layers alternating with topological insulators. In addition to superlattice structures, we envision ''inverted'' structures, in which two topological insulators sandwich between them a single superconducting $Cu_xBi_2Se_3$ layer. In a magnetic field, the two surfaces are connected by Abrikosov vortices acting as ''worm holes''. Such schemes introduce notions that should expand research on the topological surface states.

The work at Princeton was supported by the National Science Foundation MRSEC program, Grant No. DMR-0819860.

[1] J. Moore, Nature Phys. **5**, 378 (2009).
[2] J. Zaanen, Science **323**, 888 (2009).
[3] M. Buttiker, Science **325**, 278 (2009).
[4] B. A. Bernevig, T. L. Hughes, and S. C. Zhang, Science **314**, 1757 (2006).
[5] M. König *et al.*, Science **318**, 766 (2007).
[6] L. Fu and C. L. Kane, Phys. Rev. B **76**, 045302 (2007).
[7] S. Murakami, New J. Phys. **9**, 356 (2007).
[8] D. Hsieh, D. Qian, L. Wray, Y. Xia, Y. S. Hor, R. J. Cava, and M. Z. Hasan, Nature (London) **452**, 970 (2008).
[9] Y. Xia, D. Qian, D. Hsieh, L. Wray, A. Pal, A. Bansil, D. Grauer, Y. S. Hor, R. J. Cava, and M. Z. Hasan, Nature Phys. **5**, 398 (2009).
[10] Y. L. Chen *et al.*, Science **325**, 178 (2009).
[11] F. Wilczek, Nature Phys. **5**, 614 (2009).
[12] L. Fu and C. L. Kane, Phys. Rev. Lett. **100**, 096407 (2008).
[13] L. Fu and C. L. Kane, Phys. Rev. Lett. **102**, 216403 (2009).
[14] A. R. Akhmerov, J. Nilsson, and C. W. J. Beenakker, Phys. Rev. Lett. **102**, 216404 (2009).
[15] B. Seradjeh, J. E. Moore, and M. Franz, Phys. Rev. Lett. **103**, 066402 (2009).
[16] J. D. Sau, R. M. Lutchyn, S. Tewari, and S. D. Sarma, arXiv:0907.2239v2.
[17] Y. Tanaka, T. Yokoyama, and N. Nagaosa, arXiv:0907.2088v3.
[18] K. T. Law, P. A. Lee, and T. K. Ng, arXiv:0907.1909v2.
[19] H. Lind and S. Liden, Solid State Sci. **5**, 47 (2003).
[20] A. Al Bayaz, A. Giani, A. Foucaran, F. Pascal-Delannoy, and A. Boyer, Thin Solid Films **441**, 1 (2003).
[21] G. Zhang, H. Qin, J. Teng, J. Guo, Q. Guo, X. Dai, Z. Fang, and K. Wu, arXiv:0906.5306v1.
[22] E. Morosan *et al.*, Nature Phys. **2**, 544 (2006).
[23] V. P. Zhuse, V. M. Sergeeva, and E. L. Shtrum, Sov. Phys. Tech. Phys. **3**, 1925 (1958).
[24] L. P. Caywood, Jr. and G. R. Miller, Phys. Rev. B **2**, 3209 (1970).
[25] A. Vaško, L. Tichý, J. Horãk, and J. Weissenstein, Appl. Phys. **5**, 217 (1974).
[26] B. Liautard, J. C. Garcia, G. Brun, J. C. Tedenac, and M. Maurin, Eur. J. Solid State Inorg. Chem. **27**, 819 (1990).
[27] M. I. Golovej, J. V. Voroshilov, and M. V. Potorij, Izv. Vyss. Uch. Zaved., Khym I Khym. Tekh. **28**, 7 (1985).
[28] Y. S. Hor *et al.*, Phys. Rev. B **79**, 195208 (2009).
[29] J. G. Checkelsky, Y. S. Hor, M.-H. Liu, D.-X. Qu, R. J. Cava, and N. P. Ong, Phys. Rev. Lett. **103**, 246601 (2009).
[30] H. Zhang *et al.*, Nature Phys. **5**, 438 (2009).
[31] D. Hsieh *et al.*, Nature (London) **460**, 1101 (2009).